JOURNAL OF GEOPHYSICAL RESEARCH, VOL. 115, E02002, doi:10.1029/2009JE003427, 2010

Mineralogical and chemical characterization of lunar highland soils: Insights into the space weathering of soils on airless bodies

Lawrence A. Taylor,[1] Carlé Pieters,[2] Allan Patchen,[1] Dong-Hwa S. Taylor,[1] Richard V. Morris,[3] Lindsay P. Keller,[3] and David S. McKay[3]

Received 8 May 2009; revised 13 August 2009; accepted 25 September 2009; published 17 February 2010.

[1] With reflectance spectroscopy, one is measuring only properties of the fine-grained regolith most affected by space weathering. The Lunar Soil Characterization Consortium has undertaken the task of coordinated characterization of lunar soils, with respect to their mineralogical and chemical makeup. It is these lunar soils that are being used as "ground truth" for all airless bodies. Modal abundances and chemistries of minerals and glasses in the finest size fractions (20–45, 10–20, and <10 μm) of four Apollo 14 and six Apollo 16 highland soils have been determined, as well as their bulk chemistry and I_S/FeO values. Bidirectional reflectance measurements (0.3–2.6 μm) of all samples were performed in the Reflectance Experiment Laboratory. A significant fraction of nanophase Fe^0 (np-Fe^0) appears to reside in agglutinitic glasses. However, as grain size of a soil decreases, the percentage of total iron present as np-Fe^0 increases significantly, whereas the agglutinitic glass content rises only slightly; this is evidence for a large contribution to the I_S/FeO values from the surface-correlated nanophase Fe^0, particularly in the <10 μm size fraction. The compositions of the agglutinitic glasses in these fine fractions of the highland soils are different from the bulk chemistry of that size; however, compositional trends of the glasses are not the same as those observed for mare soils. It is apparent that the glasses in the highland soils contain chemical components from outside their terrains. It is proposed that the Apollo 16 soils have been adulterated by the addition of impact-transported soil components from surrounding maria.

Citation: Taylor, L. A., C. Pieters, A. Patchen, D.-H. S. Taylor, R. V. Morris, L. P. Keller, and D. S. McKay (2010), Mineralogical and chemical characterization of lunar highland soils: Insights into the space weathering of soils on airless bodies, *J. Geophys. Res.*, *115*, E02002, doi:10.1029/2009JE003427.

1. Introduction

[2] The varied processes of space weathering that occur during soil formation on the Moon are thought to be similar to those for many other airless bodies (e.g., Phobos, Eros, Mercury) although different in magnitude and cumulative effect. Therefore, the study of these effects within lunar soils should form the basis for our understanding of the regoliths on other heavenly bodies. This is a particularly applicable axiom for reflectance spectroscopy of these soils. It has been repeatedly demonstrated that it is the fine fractions (<45 μm) that dominate the spectral reflectance signatures of lunar soils [*Pieters*, 1983, 1993; *Pieters et al.*, 1993; *Hapke*, 2001]. The 10–20 μm size fraction is the most similar to the overall spectral properties of the bulk soil. However, it is also the finer size fractions that concentrate the major products of space weathering, e.g., nanophase metallic iron (np-Fe^0), which affect the overall continuum and strength of absorption features of the observed spectra.

[3] Using the Apollo and Luna lunar soils to document the products of space weathering, we have studied a selected suite of the Apollo 14 and 16 highland soils (Table 1). This study is a continuation to our characterization of the mineralogical and glassy components of the fine fractions of lunar mare soils [e.g., *Taylor et al.*, 2001a, 2001b; *Pieters et al.*, 2000, 2001], especially the complicated agglutinitic glass [*Basu et al.*, 1996; *Basu and Molinaroli*, 1999]. Specific soils were chosen for their representation of diverse degrees of maturation. These Apollo highland soils may represent a large portion of the nearside of the Moon. Many systematics of the progression of soil properties with decreasing grain size are similar to those of mare soils, which appeared to support the fusion of the finest fraction model [*Papike et al.*, 1982] for lunar soil formation. However, the relationships of the bulk composition of the size fractions for the Apollo 14 and 16 soils to that of the composition of agglutinitic glass are quite different from those for mare soils and appear to be in an opposite sense. This may necessitate modifications to the soil

[1] Planetary Geosciences Institute, Department of Earth and Planetary Sciences, University of Tennessee, Knoxville, Tennessee, USA.
[2] Department of Geological Sciences, Brown University, Providence, Rhode Island, USA.
[3] NASA Johnson Space Center, Houston, Texas, USA.

0148-0227/10/2009JE003427$09.00

Table 1. Lunar Highland Soils Studied by the Lunar Soil Characterization Consortium

Samples	Is/FeO[a]	Maturity[b]
Apollo 16		
61221	9	I
67461	25	I
67481	31	S
61141	56	S
64801	71	M
62231	91	M
Apollo 14		
14141	6	I
14163	57	M
14260	72	M
14259	85	M

[a]Values from compilation of *Morris* [1978] for the <250 μm portion of each soil.

[b]Maturity based on I_s/FeO [10]. I, Immature (<30); S, Submature (30–60); M, Mature (>60).

formation paradigm, and was first addressed by *Pieters and Taylor* [2003a].

1.1. Lunar Soil Characterization Consortium

[4] In order to document the space weathering effects on lunar spectra, the Lunar Soil Characterization Consortium (LSCC) was established [*Taylor et al.*, 1999, 2001b] for the collaborative study of lunar soils. This group of lunar soil scientists brings different expertise and instrumental techniques related to the quantification of space weathering effects and the deciphering of these effects in reflectance spectra. The members of this LSC Consortium are D. S. McKay (size separation), R. V. Morris (FMR), L. P. Keller (TEM/SEM), C. M. Pieters (spectral reflectance), and L. A. Taylor (bulk chemistry; modal characterization/mineral chemistry).

1.2. Suite of Lunar Highland Soils

[5] In a logical continuation of our soil characterization studies for mare soils, we have selected a suite of lunar highland soils to represent the diversity in soil maturities, using the concept of I_s/FeO values from *Morris* [1976]. These soils are listed in Table 1. "Pristine" samples of each of them were allocated by the Curation and Planning Team for Extra Terrestrial Materials (CAPTEM), and the curatorial staff at Johnson Space Center efficiently handled the necessary allocations. The actual sample handling logistics and allocations are presented in Figure 1 of *Taylor et al.* [2001a].

2. Methodology

2.1. Size Separation

[6] Four Apollo 14 and six Apollo 16 highland soils were sieved in the laboratory of D. S. McKay at Johnson Space Center. Triply-distilled water was used through out the process. At first, the lunar sample allocation of the <1 mm size portion of each pristine soil was sieved to obtain a <45 μm size fraction. A split of this <45 μm fraction was then sieved into the three size ranges: 20–45 μm, 10–20 μm, and <10 μm. Great care was taken to assure the size fractions retain their natural soil properties, especially grain coatings. According to the same distribution plan as utilized for the mare soils [*Taylor et al.*, 2001b], samples of each of the size splits were taken and distributed to members of the LSCC for their specific analysis.

2.2. Bulk Sample Chemical Analyses

[7] Major element chemistry was determined on portions of each size fraction. The fused bead technique was used for preparation of the samples for electron microprobe analyses. In a stream of dry nitrogen gas, approximately 5 mg of representative sample was fused on a Mo-strip heater. The samples were heated to a melt, held for 20–30 s, and quenched by rapidly reducing the heat input (i.e., turning off the current). The resulting glasses were mounted in a multiholed plastic disk, impregnated with epoxy, polished, coated with carbon, and subjected to at least 10 electron microprobe analyses per glass, using a 20 μm beam size, 15 Kv potential, and 20 nA beam current on the Cameca SX-50 EMP at the University of Tennessee.

2.3. Modal Analyses by Electron Microprobe

[8] Detailed petrographic properties of lunar highland soils, particularly the finer fractions, are poorly known. With these fine grain sizes (i.e., <45 μm), normal optical microscopic techniques, that are typically used are not efficient. Therefore, modern techniques are required to characterize soil compositions and mineral modes with the accuracy and precision needed for spectroscopic modeling. The polished grain mounts prepared by the Curatorial Staff at Johnson Space Center formed the basis for all modal and phase characterization. Using the technique presented by *Taylor et al.* [1996], accurate modal analyses were performed with an Oxford Instrument Energy Dispersive Spectrometer Unit (EDS) on a Cameca SX-50 electron microprobe at the University of Tennessee. Through use of Oxford Instruments *FeatureScan* software, it was possible to readily determine the modal proportions of minerals and glasses in thousands of fine particles in the 20–45 μm, 10–20 μm, and <10 μm size fractions of the lunar soils. This is based upon gathering energy dispersive (EDS) chemical data from 150,000–200,000 points on the phases (not epoxy) in each grain mount, thereby classifying the minerals by their chemistry. Additional programs allowed for the determination of the average chemical composition of each mineral and glass phase. The phase compositional data, as well as all our soil characterization data for both the mare and the highland soils studied by the LSCC are accessible at http://web.utk.edu/~pgi/data.html.

2.4. Difficulties in Modal Analyses of Minerals and Glasses in Highland Soils

[9] The first studies of the LSCC were performed with mare soils [*Taylor et al.*, 2001a, 2001b], and mare soils were chosen to start our characterization because they contain minerals and glasses that have vastly contrasting chemistries (e.g., pyroxene versus plagioclase versus agglutinitic glass) thereby making their identification by chemistry relatively easy. It was anticipated that applications of our mare-based, X-ray digital-imaging analysis scheme to highland soils would be considerably more difficult and time consuming than for the mare soils. This is largely due to the limited compositional range of highland soils, each with a bulk composition that approximates plagioclase feldspar with only minor mafic components (e.g., ~5 wt % FeO). These several considerations needed to be made in order to make more effective the application of our techniques to highland soils.

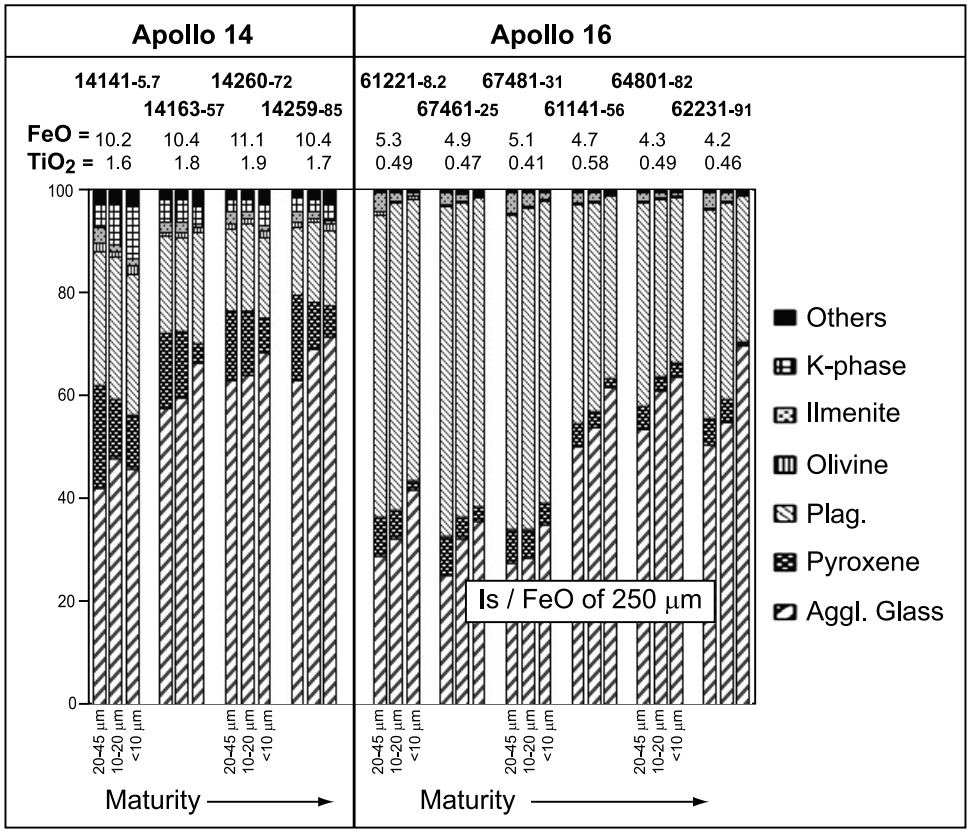

Figure 1. Modal analyses of phases in the fine fractions of highland soils. These data are modified after those in a LPSC abstract [*Taylor et al.*, 2003].

[10] The composition of the minerals and glasses in the three size fractions of the four Apollo 14 and six Apollo 16 soils (Table 1) were determined by the extensive analyses of each phase. The agglutinitic glass was especially placed in close scrutiny. Inasmuch as the composition of the agglutinitic glass in highland soils is not far removed from that of the highland bulk soil, and the bulk soil is near that of pure plagioclase, this glass closely mimics plagioclase. Therefore, experiments were conducted with the electron microprobe and the EDS unit in order to consider the several key parameters that determine the precision of the EDS X-ray analyses [*Taylor et al.*, 2001c, 2002, 2003]. For example, it was been observed that 20 kV excitation is better than the 15 kV typically used by most EMP users [*Taylor et al.*, 1996].

[11] For the highland soils, a digital map of the entire section of the grain mount is first made, and many agglutinates, displaying vesicular texture, as well as other phases, are optically identified by reflected light microscopy. The initial examination with the EMP consists of wavelength dispersive spectral (WDS) EMP determinations of the compositional limits of all the optically identified minerals and glasses from direct analyses of ~1000–3000 phases, in particular the agglutinitic glasses. With a given soil, it is necessary to perform such initial characterization, for even subtle differences in chemistry can change the "chemical windows" for a mineral or glass. In particular, the agglutinitic glasses are all alumina-rich, but the agglutinitic glass, and the minor amount of nonagglutinitic impact glass, can be distinguished from plagioclase (including maskelynite) by their FeO and MgO contents. As demonstrated by *McGee* [1993], all lunar highland plagioclase contains <0.5 wt % FeO and <0.5 wt % MgO. We verified this for the identified agglutinitic and impact glasses. These glasses then formed the compositional basis for our EDS modal analyses.

[12] In this study, nonagglutinitic, impact-produced glasses are also reported as agglutinitic glass, since the compositions from our analyses appear similar and because most of the impact-produced glasses in the fine grain sizes examined in this study contain np-Fe^0. In the modal values for agglutinitic glass, we estimate that the other nonagglutinitic, impact glasses usually consist of <10% of the glass present. There is no doubt that some small amount of "nonagglutinitic (i.e., impact) glasses" might have been included, particularly in the finest grain size.

2.5. Ferromagnetic Resonance Analyses

[13] The detection and analyses of the abundances of single-domain np-Fe^0 were determined by Ferromagnetic Resonance (FMR) measurements performed in the Magnetics Lab of R.V. Morris, at Johnson Space Center. It has been in this laboratory that virtually all the FMR measurements on lunar samples have been made since 1972, ensuring consistency, accuracy, and precision.

3. Modal Analyses of Minerals and Glasses

[14] The modal abundances of 12 different minerals and glasses were determined on polished grain mounts of each of the 30 size splits (10 soils X 3 sizes). This was performed

Table 2. Modal Abundance of Minerals and Glasses in Finest Size Fractions of Selected Apollo Highland Soils[a]

	14141-5.7			14163-57			14260-72			14259-85		
	20–45 μm	10–20 μm	<10 μm	20–45 μm	10–20 μm	<10 μm	20–45 μm	10–20 μm	<10 μm	20–45 μm	10–20 μm	<10 μm
Agglutinitic Glass	41.0	48.6	45.9	56.4	58.5	66.3	64.0	65.2	66.5	60.5	68.7	71.6
Pyroxene	19.8	10.9	10.3	16.2	13.8	3.8	13.7	12.1	7.7	18.2	9.1	5.9
Plagioclase	26.6	28.0	27.6	18.9	18.3	21.8	15.6	16.1	16.3	14.1	15.4	14.6
Olivine	4.0	1.6	1.5	2.4	2.1	0.4	2.1	1.5	1.4	2.3	1.4	0.7
Ilmenite	1.9	1.1	1.7	0.8	0.9	1.1	0.9	1.0	1.3	1.3	1.2	1.5
K Phases	4.5	7.4	10.8	3.8	4.1	3.4	2.5	2.6	3.7	2.5	2.7	3.4
Others	2.2	2.4	2.2	1.5	2.3	3.2	1.2	1.5	3.1	1.1	1.5	2.3
Total	100.0	100.0	100.0	100.0	100.0	100.0	100.0	100.0	100.0	100.0	100.0	100.0
	61221-9.2			67461-25			67481-31			61141-56		
	20–45 μm	10–20 μm	<10 μm	20–45 μm	10–20 μm	<10 μm	20–45 μm	10–20 μm	<10 μm	20–45 μm	10–20 μm	<10 μm
Agglutinitic Glass	28.9	32.6	41.6	25.4	32.4	35.8	27.6	28.6	35.2	50.1	53.9	61.6
Pyroxene	7.4	5.3	1.5	7.3	4.1	2.8	6.6	5.6	3.6	4.4	3.3	1.7
Plagioclase	58.7	59.4	54.4	64.3	61.0	60.0	61.2	62.0	58.8	42.5	40.3	35.3
Olivine	3.9	2.0	0.9	2.5	1.5	0.7	4.0	2.9	1.5	2.1	1.6	0.5
Ilmenite	0.6	0.3	0.9	0.3	0.3	0.2	0.1	0.2	0.2	0.3	0.3	0.3
K Phases	0.2	0.2	0.3	0.1	0.2	0.1	0.3	0.4	0.3	0.3	0.4	0.3
Others	0.3	0.2	0.4	0.1	0.5	0.4	0.2	0.3	0.4	0.3	0.2	0.3
Total	100.0	100.0	100.0	100.0	100.0	100.0	100.0	100.0	100.0	100.0	100.0	100.0
	64801-82			62231-91								
	20–45 μm	10–20 μm	<10 μm	20–45 μm	10–20 μm	<10 μm						
Agglutinitic Glass	53.6	61.0	63.6	50.6	55.0	69.5						
Pyroxene	4.5	2.8	2.7	5.1	4.40	0.9						
Plagioclase	39.3	34.5	32.3	40.5	37.8	28.3						
Olivine	1.8	1.0	0.6	2.9	1.7	0.3						
Ilmenite	0.3	0.2	0.2	0.3	0.5	0.4						
K Phases	0.3	0.3	0.4	0.3	0.4	0.3						
Others	0.2	0.2	0.2	0.3	0.2	0.3						
Total	100.0	100.0	100.0	100.0	100.0	100.0						

[a]Maturity as I_S/FeO of the <250 μm fraction [*Morris*, 1978] is given directly after the soil number, a value commonly used as the reference maturity for an entire soil.

utilizing the X-ray digital imaging technique outlined by *Taylor et al.* [1996], with several modifications detailed above. The modal data for the major phases in the Apollo 14 and 16 soils are given in Table 2 and graphically shown in Figure 1. The pyroxene values are for total pyroxene, calculated by combining abundances of the four different pyroxene compositions that were determined. The actual breakdown of these total pyroxene abundances is given in Table 3. It should be noticed that a designation has been made for a "K phase", which is for the "KREEPY" phases (e.g.,

Table 3. Modal Percentages of Four Subsets of Pyroxenes in the Finest Size Fractions of Apollo Highland Soils[a]

	14141-5.7			14163-57			14260-72			14259-85		
	20–45 μm	10–20 μm	<10 μm	20–45 μm	10–20 μm	<10 μm	20–45 μm	10–20 μm	<10 μm	20–45 μm	10–20 μm	<10 μm
Orthopyroxene	7.57	4.07	3.37	6.50	5.68	1.51	4.68	5.14	2.58	7.40	3.72	1.92
Pigeonite	8.08	4.58	4.29	5.66	4.94	1.38	4.99	4.23	3.15	6.14	3.18	1.96
Mg-Clinopyroxene	3.08	1.85	2.19	3.10	2.41	0.91	3.07	2.00	1.51	3.04	1.66	1.77
Fe-Pyroxene	1.08	0.38	0.44	0.92	0.78	0.14	0.94	0.64	0.48	1.57	0.50	0.29
Total Pyroxene	19.81	10.88	10.29	16.18	13.81	3.94	13.68	12.01	7.72	18.15	9.06	5.94
	61221-9.2			67461-25			67481-31			61141-56		
	20–45 μm	10–20 μm	<10 μm	20–45 μm	10–20 μm	<10 μm	20–45 μm	10–20 μm	<10 μm	20–45 μm	10–20 μm	<10 μm
Orthopyroxene	2.96	1.82	0.56	2.96	1.47	1.09	2.95	2.55	1.38	1.68	1.69	0.22
Pigeonite	2.24	1.43	0.55	1.61	1.07	0.64	1.54	1.27	1.05	1.38	2.15	0.23
Mg-Clinopyroxene	1.98	1.95	0.37	2.53	1.52	1.06	1.94	1.73	1.41	1.11	1.45	0.19
Fe-Pyroxene	0.19	0.14	0.02	0.18	0.05	0.04	0.17	0.13	0.05	0.18	0.04	0.06
Total Pyroxene	7.37	5.34	1.50	7.28	4.11	2.83	6.60	5.68	3.89	4.35	5.33	0.70
	64801-82			62231-91								
	20–45 μm	10–20 μm	<10 μm	20–45 μm	10–20 μm	<10 μm						
Orthopyroxene	2.03	1.24	1.18	2.08	1.99	0.28						
Pigeonite	1.15	0.96	0.84	1.33	1.55	0.27						
Mg-Clinopyroxene	1.33	0.60	0.64	1.52	1.74	0.30						
Fe-Pyroxene	0.01	0.01	0.00	0.19	0.12	0.03						
Total Pyroxene	4.52	2.81	2.66	5.12	5.40	0.88						

[a]Maturity as I_s/FeO of the <250 μm fraction [*Morris*, 1978] is given directly after the soil number, a value commonly used as the reference maturity for an entire soil.

Table 4. Bulk Chemistry and I_s/FeO Values of the Finest Size Fractions of Apollo Highland Soils[a]

	14141-5.7				14163-57				14260-72			
	<45 μm	20–45 μm	10–20 μm	<10 μm	<45 μm	20–45 μm	10–20 μm	<10 μm	<45 μm	20–45 μm	10–20 μm	<10 μm
SiO_2	47.9	47.2	48.4	49.2	47.4	47.1	47.4	47.2	47.6	47.4	47.5	47.8
TiO_2	1.65	1.96	1.71	1.51	1.90	2.00	1.88	2.07	1.85	1.86	1.98	1.94
Al_2O_3	17.0	15.0	17.2	19.2	17.1	15.4	17.0	18.9	17.3	16.3	17.3	19.1
Cr_2O_3	0.22	0.26	0.23	0.21	0.20	0.23	0.22	0.21	0.21	0.22	0.23	0.20
MgO	9.28	11.0	9.08	6.99	9.49	11.0	9.57	8.14	9.46	10.4	9.53	8.21
CaO	10.7	10.1	10.7	11.3	10.9	10.2	10.8	11.6	11.0	10.7	11.0	11.8
MnO	0.14	0.15	0.13	0.10	0.15	0.15	0.13	0.12	0.15	0.14	0.13	0.12
FeO	9.81	11.6	9.46	7.66	9.94	11.5	10.1	8.83	9.65	10.7	9.84	8.10
Na_2O	0.76	0.59	0.71	0.91	0.65	0.57	0.67	0.70	0.61	0.60	0.60	0.57
K_2O	0.70	0.47	0.66	0.96	0.51	0.41	0.51	0.55	0.49	0.44	0.46	0.47
P_2O_5	0.50	0.26	0.32	0.40	0.35	0.21	0.27	0.33	0.32	0.22	0.21	0.17
SO_3	0.10	0.07	0.07	0.10	0.10	0.08	0.10	0.11	0.12	0.10	0.10	0.09
Total	98.82	98.78	98.68	98.61	98.69	99.02	98.72	98.85	98.81	99.13	98.97	98.76
I_s/FeO	9.7	5.8	11.6	14.5	66.5	43.2	64.8	87.0	93.3	80.2	98.9	144.9
	14259-85				61221-9.2				67461-25			
	<45 μm	20–45 μm	10–20 μm	<10 μm	<45 μm	20–45 μm	10–20 μm	<10 μm	<45 μm	20–45 μm	10–20 μm	<10 μm
SiO_2	47.7	47.1	47.5	47.9	44.7	44.5	44.5	44.5	44.6	44.4	44.1	44.5
TiO_2	1.80	1.99	1.96	2.02	0.52	0.56	0.54	0.50	0.35	0.44	0.39	0.34
Al_2O_3	17.4	15.8	17.4	19.3	27.3	27.2	27.5	28.5	28.4	27.3	27.8	29.4
Cr_2O_3	0.20	0.24	0.23	0.20	0.09	0.09	0.09	0.08	0.08	0.09	0.08	0.08
MgO	9.47	10.7	9.44	8.09	5.29	5.45	5.16	4.35	4.46	5.11	4.80	3.83
CaO	11.1	10.5	11.0	11.9	15.9	15.9	16.0	16.5	16.5	16.1	16.5	17.1
MnO	0.13	0.15	0.13	0.12	0.08	0.06	0.05	0.06	0.06	0.07	0.08	0.06
FeO	9.54	11.0	9.71	7.82	4.47	4.62	4.40	3.64	4.24	4.93	4.64	3.35
Na_2O	0.62	0.60	0.63	0.63	0.48	0.46	0.45	0.53	0.40	0.41	0.39	0.43
K_2O	0.47	0.43	0.47	0.50	0.09	0.07	0.09	0.13	0.06	0.05	0.05	0.07
P_2O_5	0.30	0.26	0.23	0.23	0.06	0.05	0.05	0.06	0.04	0.03	0.04	0.03
SO_3	0.11	0.09	0.12	0.10	0.07	0.04	0.06	0.10	0.06	0.07	0.04	0.07
Total	98.80	99.02	98.87	98.84	99.13	99.07	98.93	99.00	99.26	99.00	98.90	99.31
I_s/FeO	108.6	77.2	101.8	174.8	13.6	8.4	13.89	19.8	29.8	22.3	23.9	35.2
	67481-31				61141-56				64801-82			
	<45 μm	20–45 μm	10–20 μm	<10 μm	<45 μm	20–45 μm	10–20 μm	<10 μm	<45 μm	20–45 μm	10–20 μm	<10 μm
SiO_2	44.6	44.7	44.4	44.5	45.0	44.5	44.6	44.9	45.0	44.6	44.5	44.8
TiO_2	0.44	0.49	0.40	0.42	0.59	0.58	0.64	0.59	0.65	0.63	0.68	0.61
Al_2O_3	28.1	26.7	28.4	29.1	26.3	26.1	25.6	27.4	26.9	26.5	26.3	27.7
Cr_2O_3	0.10	0.09	0.09	0.08	0.12	0.11	0.13	0.11	0.10	0.10	0.12	0.12
MgO	4.91	5.98	4.54	4.09	6.39	6.56	6.84	5.53	5.83	6.09	6.18	5.22
CaO	16.2	15.6	16.4	16.7	15.3	15.2	15.2	16.0	15.6	15.6	15.6	16.1
MnO	0.06	0.08	0.05	0.07	0.07	0.08	0.08	0.07	0.06	0.08	0.08	0.07
FeO	4.38	5.19	4.04	3.61	4.80	5.15	5.14	3.66	4.68	4.82	4.78	3.84
Na_2O	0.43	0.45	0.45	0.46	0.43	0.46	0.41	0.48	0.43	0.44	0.41	0.42
K_2O	0.06	0.06	0.07	0.08	0.11	0.10	0.10	0.14	0.12	0.12	0.11	0.14
P_2O_5	0.04	0.05	0.04	0.04	0.06	0.06	0.05	0.06	0.07	0.06	0.06	0.04
SO_3	0.04	0.04	0.06	0.07	0.09	0.05	0.08	0.11	0.09	0.10	0.07	0.11
Total	99.39	99.50	99.08	99.22	99.34	99.00	98.91	99.11	99.50	99.20	98.99	99.21
I_s/FeO	33.5	20.7	33.0	38.5	94.5	75.5	81.6	119.3	92.2	83.4	84.9	115.2
	62231-91											
	<45 μm	20–45 μm	10–20 μm	<10 μm								
SiO_2	45.0	44.5	44.7	45.0								
TiO_2	0.60	0.58	0.61	0.58								
Al_2O_3	26.3	25.7	26.3	27.4								
Cr_2O_3	0.11	0.11	0.13	0.13								
MgO	6.20	6.59	6.38	5.49								
CaO	15.4	15.3	15.5	16.1								
MnO	0.09	0.09	0.07	0.07								
FeO	4.87	5.31	4.86	3.63								
Na_2O	0.43	0.42	0.41	0.46								
K_2O	0.12	0.09	0.10	0.14								
P_2O_5	0.07	0.07	0.05	0.04								
SO_3	0.09	0.08	0.08	0.13								
Total	99.32	98.87	99.22	99.22								
I_s/FeO	116.7	80.7	109.9	169.0								

[a]The chemistry was determined by EMP analyses of fused beads of the soil. Values of I_s/FeO are from FMR analyses. Maturity as I_s/FeO of the <250 μm fraction [*Morris*, 1978] is given directly after the soil number, a value commonly used as the reference maturity for an entire soil.

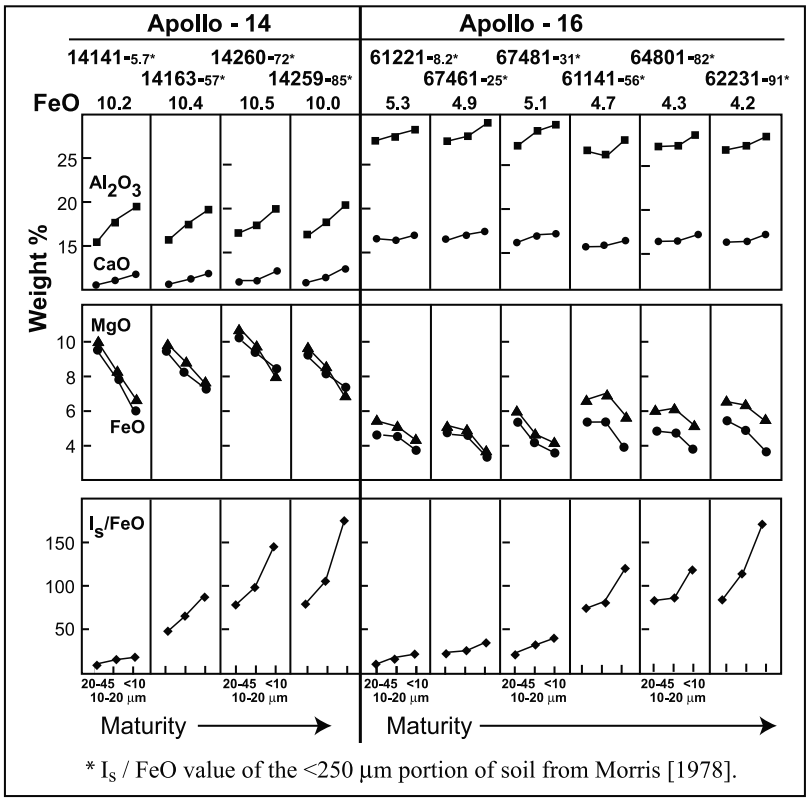

Figure 2. Comparisons of oxide components of the bulk chemistry of the fine fractions of highland soils in addition to their I_S/FeO values.

K-rich feldspar; K-rich glasses) typically associated with the Apollo 14 soils. The compositions of the minerals and agglutinitic glass in the size fractions of these Apollo soil are given in Table 4.

[15] As shown by comparison of different soils in Figure 1, there is an overall increase in the abundance of agglutinitic glass as the soils mature, from low to high I_S/FeO values. This correlates with the general decrease in the amounts of the minerals and is to be expected, since the longer the exposure of soil on the surface of the Moon, the greater the effects of micrometeorite gardening and general space weathering [*Taylor and McKay*, 1992]. This extended presence at the lunar surface results in an increase in the melted products (i.e., agglutinates, agglutinitic glass, and vapor-deposited patinas), due to the impacting processes.

[16] Within a given soil, a similar scheme is apparent from larger to finer size fractions. With decrease in grain size, the abundances of the agglutinitic glasses increase (with the exception of the <10 μm fraction of 14141-5.7). Although there is also a tendency for the plagioclase to slightly increase in the finer fractions, there are distinct decreases in pyroxene and olivine with decreasing grain size. Therefore, the ferromagnesian minerals decrease proportionately, while the plagioclase abundances stay constant or increase slightly. These trends are also apparent with the bulk chemistry of the various size fractions, as presented below.

[17] The designation of ilmenite in the modes includes minor amounts of Ti-Cr-rich spinels (<1%). Although low in abundance (i.e., <2%), ilmenite in the Apollo 14 soils, in particular, shows a general slight increase with decreasing grain size (Table 2), contrary to that in mare soils [*Taylor et al.*, 2001a, 2001b]. These observations for the Apollo 14 and 16 soils, some of which were also seen with the mare soils, are addressed by Pieters and Taylor [*Pieters and Taylor*, 2002, 2003a, 2003b].

4. Soil Chemistry

[18] Several systematic changes can be readily observed in Figure 2 and Table 4 with respect to the bulk chemistry of each of the size fractions of the highland soils. The composition of a lunar highland soil systematically changes as a function of grain size. With a decrease in grain size, the soils (1) increase in plagioclase components (e.g., CaO, Al_2O_3) and (2) decrease in olivine and pyroxene components (e.g., FeO, MgO). It appears that similar soil formational processes may occur in the highlands as in the maria. That is, the finest fractions of both the mare and Apollo 14 and 16 soils become enriched in plagioclase components. This observation for the mare soils originally led us to conclude [*Taylor et al.*, 2001a, 2001b] that the data appeared to support the fusion of the finest fraction model of agglutinate formation by *Papike et al.* [1982].

[19] There is a systematic and predictable increase of I_S/FeO with decreasing grain size, a result of the increased presence of single-domain, np-Fe^0, as originally observed by *Morris* [1978]. Although the absolute amount of FeO decreases in the finer fractions, the percentage of this iron that is present in the metallic Fe^0 state as np-Fe^0 increases

Table 5. Average Compositions of Minerals and Glasses in the Finest Size Fractions of Apollo Highland Soils[a]

	Plagioclase	Ilmenite	Olivine	K Glass	Agglutinitic Glass	Orthopyroxene	Pigeonite	Mg- Clinopyroxene	Fe- Clinopyroxene
					14141-5.7 (20–45 μm)				
SiO_2	45.7	<0.04	36.2	70.1	47.0 (37)	52.8	51.6	49.9	46.9
TiO_2	<0.04	52.4	0.07	0.27	1.82 (208)	0.68	0.74	1.30	1.06
Al_2O_3	33.5	0.10	0.06	13.7	17.9 (75)	1.03	1.51	1.74	1.32
Cr_2O_3	<0.04	0.61	0.08	<0.04	0.18 (11)	0.36	0.47	0.46	0.21
MgO	0.09	3.42	31.8	0.31	7.98 (441)	24.6	20.5	13.8	6.72
CaO	17.6	0.17	0.15	1.16	11.4 (34)	1.84	4.59	15.1	10.3
FeO	0.06	40.8	30.1	1.21	9.76 (608)	17.3	19.0	16.0	30.9
Na_2O	1.22	<0.04	<0.04	0.86	0.74 (51)	<0.04	<0.04	0.07	<0.04
K_2O	0.16	<0.04	<0.04	8.81	0.46 (54)	<0.04	<0.04	<0.04	<0.04
Total	98.33	97.50	98.46	96.42	97.24	98.61	98.41	98.37	97.41
					14141-5.7 (10–20 μm)				
SiO_2	45.2	<0.04	36.6	72.0	46.8 (41)	52.7	51.7	50.0	46.7
TiO_2	0.06	52.3	0.11	0.39	1.69 (180)	0.76	0.78	1.51	1.23
Al_2O_3	34.0	0.14	0.14	12.1	19.3 (64)	1.02	1.37	1.98	1.39
Cr_2O_3	<0.04	0.56	0.08	<0.04	0.20 (12)	0.34	0.45	0.56	0.18
MgO	0.13	3.33	32.8	0.12	7.91 (369)	24.2	20.6	14.6	5.73
CaO	18.0	0.20	0.15	1.96	11.9 (32)	1.99	4.33	16.2	10.6
FeO	0.17	40.6	28.9	3.31	8.81 (417)	17.4	19.2	13.0	31.8
Na_2O	1.07	<0.04	<0.04	1.49	0.74 (59)	<0.04	<0.04	0.10	<0.04
K_2O	0.15	0.05	<0.04	5.45	0.39 (41)	<0.04	<0.04	<0.04	<0.04
Total	98.78	97.18	98.78	96.82	97.80	98.41	98.43	97.95	97.63
					14163-57 (20–45 μm)				
SiO_2	46.2	<0.04	36.7	67.6	46.8 (30)	52.9	51.5	50.6	46.8
TiO_2	0.04	51.6	0.08	0.43	1.71 (138)	0.75	0.67	1.27	0.94
Al_2O_3	32.9	0.16	0.04	14.8	17.2 (61)	1.30	1.46	1.70	1.01
Cr_2O_3	<0.04	0.65	0.05	<0.04	0.17 (13)	0.32	0.39	0.39	0.12
MgO	0.04	2.17	34.3	0.54	8.64 (394)	24.2	18.1	13.9	4.97
CaO	17.6	0.25	0.16	2.25	11.4 (28)	2.00	5.17	16.6	11.0
FeO	0.06	42.3	26.8	1.90	10.2 (49)	16.8	21.0	13.8	32.7
Na_2O	1.38	<0.04	<0.04	1.21	0.58 (39)	<0.04	0.04	0.13	0.05
K_2O	0.18	0.04	<0.04	8.40	0.43 (44)	<0.04	<0.04	<0.04	<0.04
Total	98.4	97.17	98.13	97.13	97.03	98.27	98.33	98.39	97.59
					14163-57 (10–20 μm)				
SiO_2	45.8	0.12	36.8	67.9	46.4 (28)	52.9	51.4	50.4	47.6
TiO_2	<0.04	52.0	0.08	0.30	1.66 (123)	0.75	0.68	1.38	1.04
Al_2O_3	33.6	0.19	0.09	15.2	18.1 (63)	1.10	1.18	1.90	1.24
Cr_2O_3	<0.04	0.45	0.11	<0.04	0.19 (37)	0.31	0.38	0.48	0.18
MgO	0.08	3.95	33.3	0.14	8.64 (353)	24.8	19.4	14.7	7.52
CaO	17.6	0.26	0.24	1.73	11.6 (28)	1.88	4.68	17.2	10.8
FeO	0.22	39.5	27.9	1.83	9.65 (438)	16.4	20.3	12.1	29.0
Na_2O	1.33	<0.04	<0.04	1.23	0.59 (40)	<0.04	<0.04	0.13	0.06
K_2O	0.14	<0.04	<0.04	8.64	0.36 (39)	<0.04	<0.04	<0.04	<0.04
Total	98.77	96.47	98.52	96.97	97.19	98.14	98.02	98.29	97.44
					14260-72 (20–45 μm)				
SiO_2	45.6	0.07	36.7	68.6	46.3 (37)	52.8	50.9	50.1	47.1
TiO_2	0.05	52.4	0.09	0.38	1.54 (113)	0.79	0.88	1.50	1.01
Al_2O_3	33.7	0.06	0.05	15.8	18.6 (66)	1.06	1.63	2.10	1.15
Cr_2O_3	<0.04	0.50	0.12	<0.04	0.21 (15)	0.35	0.47	0.58	0.24
MgO	0.09	3.54	32.8	0.10	8.42 (418)	24.5	18.3	14.7	6.91
CaO	17.6	0.19	0.17	2.07	11.6 (31)	1.86	5.28	16.6	12.3
FeO	0.18	40.5	29.1	0.27	9.64 (487)	17.3	21.1	12.6	28.6
Na_2O	1.22	<0.04	<0.04	1.09	0.60 (45)	<0.04	<0.04	0.12	0.0
K_2O	0.14	<0.04	<0.04	8.96	0.41 (45)	<0.04	<0.04	<0.04	<0.04
Total	98.58	97.26	99.03	97.27	97.26	98.66	98.56	98.30	97.31
					14260-72 (10–20 μm)				
SiO_2	45.8	0.10	36.9	66.3	45.5 (44)	53.0	51.1	50.8	47.8
TiO_2	0.05	51.3	0.10	0.32	1.62 (125)	0.80	0.82	1.30	1.12
Al_2O_3	33.8	0.18	0.08	15.6	19.9 (71)	1.04	1.17	1.89	1.37
Cr_2O_3	<0.04	0.53	0.09	<0.04	0.22 (11)	0.32	0.33	0.50	0.18
MgO	0.08	3.25	32.9	0.61	8.39 (401)	24.1	18.6	15.0	7.01
CaO	17.6	0.24	0.19	2.31	12.4 (34)	1.92	4.94	16.4	12.7
FeO	0.28	40.8	29.2	2.05	8.85 (434)	17.9	21.4	12.9	28.1
Na_2O	1.28	<0.04	<0.04	0.79	0.53 (42)	<0.04	<0.04	0.08	<0.04
K_2O	0.15	0.06	<0.04	8.42	0.40 (48)	<0.04	<0.04	<0.04	<0.04
Total	99.04	97.46	99.46	96.40	97.90	99.08	98.36	98.87	98.28
					14259-85 (20–45 μm)				
SiO_2	46.3	<0.04	36.9	68.7	46.5 (33)	53.0	51.4	50.3	46.9
TiO_2	0.05	52.8	0.10	0.69	1.50 (118)	0.75	0.75	1.42	1.01
Al_2O_3	33.5	0.09	0.06	14.8	19.2 (63)	0.98	1.22	2.00	1.09
Cr_2O_3	<0.04	0.52	0.11	<0.04	0.19 (11)	0.35	0.44	0.53	0.19
MgO	0.10	3.23	33.1	0.21	8.38 (378)	24.5	19.0	14.6	5.03
CaO	17.3	0.11	0.18	1.82	12.0 (29)	1.83	5.10	16.2	11.2
FeO	0.05	41.1	28.8	1.30	9.17 (459)	17.5	20.7	13.3	32.5
Na_2O	1.41	<0.04	<0.04	1.02	0.61 (66)	<0.04	<0.04	0.11	<0.04
K_2O	0.20	<0.04	<0.04	8.57	0.37 (43)	<0.04	<0.04	<0.04	<0.04
Total	98.91	97.85	99.25	97.11	97.80	98.91	98.61	98.46	97.92

Table 5. (continued)

	Plagioclase	Ilmenite	Olivine	K Glass	Agglutinitic Glass	Orthopyroxene	Pigeonite	Mg- Clinopyroxene	Fe- Clinopyroxene
					14259-85 (10–20 μm)				
SiO_2	45.8	0.08	36.8	72.8	45.8 (31)	52.4	50.9	50.2	46.8
TiO_2	<0.04	52.4	0.05	0.45	1.64 (135)	0.90	0.77	0.92	0.99
Al_2O_3	33.5	0.11	0.05	11.8	18.7 (57)	1.02	1.11	2.68	1.21
Cr_2O_3	<0.04	0.42	<0.04	<0.04	0.16 (11)	0.27	0.32	0.73	0.18
MgO	0.05	3.63	33.3	0.09	8.33 (291)	23.5	18.4	15.4	5.81
CaO	17.4	0.16	0.16	1.24	11.8 (24)	1.93	4.83	14.4	12.2
FeO	0.10	39.6	27.7	2.16	9.81 (445)	17.7	21.1	13.6	29.5
Na_2O	1.34	<0.04	<0.04	0.73	0.55 (40)	<0.04	<0.04	0.07	0.05
K_2O	0.10	<0.04	<0.04	7.49	0.36 (39)	<0.04	<0.04	<0.04	<0.04
Total	98.29	96.40	98.06	96.76	97.09	97.72	97.43	98.00	96.74
					61221-9.2 (20–45 μm)				
SiO_2	44.2	<0.04	37.7	46.4	45.1 (31)	53.0	51.6	50.8	45.0
TiO_2	<0.04	52.9	0.08	0.91	1.12 (185)	0.61	0.78	1.37	0.78
Al_2O_3	35.3	0.18	0.15	1.10	24.2 (80)	1.06	1.22	1.99	0.95
Cr_2O_3	<0.04	0.47	<0.04	<0.04	0.09 (13)	0.29	0.27	0.52	<0.04
MgO	<0.04	2.88	36.8	0.68	6.57 (485)	24.4	19.6	14.8	0.68
CaO	19.0	0.09	0.11	18.9	14.3 (35)	1.56	4.78	18.1	7.69
FeO	0.07	41.1	24.5	30.1	6.24 (557)	18.0	20.4	11.4	42.4
Na_2O	0.56	<0.04	<0.04	0.14	0.54 (42)	<0.04	0.05	0.09	<0.04
K_2O	<0.04	<0.04	<0.04	<0.04	0.16 (29)	<0.04	<0.04	<0.04	<0.04
Total	99.13	97.62	99.34	98.23	98.30	98.92	98.70	99.07	97.50
					61221-9.2 (10–20 μm)				
SiO_2	44.1	0.08	38.0	65.9	45.3 (41)	53.3	51.9	51.0	48.6
TiO_2	<0.04	51.8	0.07	1.16	1.00 (170)	0.60	0.68	1.01	0.89
Al_2O_3	34.9	0.10	0.08	12.1	23.1 (77)	0.95	1.16	1.48	1.11
Cr_2O_3	<0.04	0.44	0.05	0.08	0.13 (15)	0.34	0.36	0.42	0.14
MgO	0.07	2.57	37.0	1.58	7.37 (484)	24.8	20.4	14.6	8.37
CaO	19.1	0.42	0.19	2.69	13.9 (36)	1.65	4.01	18.7	14.3
FeO	0.16	41.9	24.0	4.66	6.98 (545)	17.64	20.4	11.4	24.8
Na_2O	0.58	<0.04	<0.04	1.42	0.43 (34)	<0.04	<0.04	0.07	0.07
K_2O	0.04	0.05	<0.04	6.37	0.14 (26)	<0.04	<0.04	<0.04	<0.04
Total	98.95	97.36	99.39	95.96	98.37	99.28	98.91	98.68	98.28
					67461-25 (20–45 μm)				
SiO_2	44.0	0.04	36.1	72.7	43.9 (43)	53.3	52.1	50.5	46.4
TiO_2	<0.04	52.4	0.06	0.35	0.53 (55)	0.56	0.51	1.06	0.82
Al_2O_3	35.0	0.07	<0.04	9.74	24.6 (79)	0.99	1.27	1.53	0.72
Cr_2O_3	<0.04	0.20	0.04	<0.04	0.15 (48)	0.38	0.42	0.56	0.05
MgO	0.06	2.33	30.9	0.12	7.47 (547)	25.4	22.3	14.3	4.01
CaO	19.2	0.22	0.11	0.47	14.6 (37)	1.52	4.51	19.0	15.7
FeO	0.15	42.4	31.9	5.26	6.48 (481)	16.9	17.3	11.5	28.0
Na_2O	0.54	<0.04	<0.04	0.11	0.40 (24)	<0.04	<0.04	0.06	0.04
K_2O	<0.04	<0.04	<0.04	7.11	0.08 (17)	<0.04	<0.04	<0.04	-
Total	98.95	97.66	99.11	95.86	98.26	99.05	98.41	98.51	95.74
					67461-25 (10–20 μm)				
SiO_2	44.3	0.04	36.6	73.4	43.7 (48)	52.7	51.9	50.8	47.5
TiO_2	<0.04	52.7	0.05	0.35	0.55 (35)	0.51	0.55	1.01	0.83
Al_2O_3	34.6	0.09	<0.04	9.92	24.9 (67)	0.79	1.36	1.43	0.75
Cr_2O_3	<0.04	0.22	0.04	<0.04	0.15 (23)	0.43	0.43	0.53	0.05
MgO	0.07	2.38	31.0	0.10	7.28 (497)	25.6	22.9	14.8	4.21
CaO	19.3	0.23	0.11	0.42	13.9 (47)	1.15	4.54	18.6	15.8
FeO	0.18	42.7	31.7	5.12	6.63 (453)	16.7	17.0	11.4	29.5
Na_2O	0.55	<0.04	<0.04	0.13	0.36 (19)	<0.04	<0.04	0.05	0.04
K_2O	<0.04	<0.04	<0.04	7.81	0.07 (11)	<0.04	<0.04	<0.04	-
Total	99.00	98.36	99.50	97.25	97.54	97.88	98.68	98.62	98.64
					67481-31 (20–45 μm)				
SiO_2	44.2	0.09	36.9	68.9	44.3 (36)	52.6	52.8	51.1	47.6
TiO_2	<0.04	53.1	0.08	0.27	0.76 (301)	0.53	0.59	1.14	1.33
Al_2O_3	35.0	<0.04	0.08	15.3	25.6 (69)	0.85	0.85	1.51	0.79
Cr_2O_3	<0.04	0.23	0.06	<0.04	0.14 (15)	0.33	0.32	0.55	0.17
MgO	0.06	2.81	33.1	0.10	6.53 (502)	23.3	22.2	14.3	4.49
CaO	19.1	0.10	0.07	1.31	15.1 (35)	1.40	4.42	18.5	17.1
FeO	0.06	42.6	29.3	0.09	5.59 (490)	19.9	18.0	11.9	27.1
Na_2O	0.56	0.04	<0.04	0.32	0.43 (22)	<0.04	<0.04	0.09	0.11
K_2O	0.06	0.04	<0.04	10.7	0.08 (10)	<0.04	<0.04	<0.04	<0.04
Total	99.04	99.01	99.59	96.99	98.51	98.91	99.18	99.09	98.69
					67481-31 (10–20 μm)				
SiO_2	44.6	0.07	37.1	70.5	44.5 (38)	53.1	53.1	51.7	48.4
TiO_2	<0.04	52.8	0.07	0.37	0.85 (138)	0.59	0.61	0.94	0.90
Al_2O_3	34.6	<0.04	<0.04	14.3	24.6 (69)	0.79	0.96	1.30	0.70
Cr_2O_3	<0.04	0.31	0.07	<0.04	0.13 (13)	0.34	0.31	0.44	0.05
MgO	0.08	2.58	33.9	<0.04	7.03 (446)	24.3	22.0	14.9	5.04
CaO	18.9	0.25	0.14	1.71	14.7 (32)	1.69	3.96	19.3	16.8
FeO	0.15	42.0	28.2	0.43	6.20 (468)	18.3	18.8	10.8	26.6

Table 5. (continued)

	Plagioclase	Ilmenite	Olivine	K Glass	Agglutinitic Glass	Orthopyroxene	Pigeonite	Mg- Clinopyroxene	Fe- Clinopyroxene
Na_2O	0.65	<0.04	<0.04	0.67	0.44 (54)	<0.04	<0.04	0.05	0.06
K_2O	0.06	<0.04	<0.04	9.11	0.18 (73)	<0.04	<0.04	<0.04	<0.04
Total	99.04	98.01	99.48	97.09	98.64	99.11	99.74	99.43	98.55
					61141-56 (20–45 μm)				
SiO_2	44.3	<0.04	37.7	71.5	44.2 (41)	52.8	52.2	51.4	45.2
TiO_2	<0.04	53.4	0.06	0.35	1.05 (169)	0.66	0.61	0.85	0.89
Al_2O_3	34.9	0.06	0.06	14.4	23.5 (83)	0.86	0.97	1.29	0.87
Cr_2O_3	<0.04	0.38	0.07	<0.04	0.16 (16)	0.33	0.33	0.40	0.08
MgO	0.04	3.78	37.7	0.15	7.52 (516)	24.6	21.3	15.1	0.69
CaO	18.9	0.13	0.11	1.55	14.3 (37)	1.61	4.62	20.0	10.4
FeO	0.10	40.8	23.5	0.68	7.17 (583)	18.0	18.8	9.57	39.8
Na_2O	0.70	<0.04	<0.04	0.86	0.40 (28)	<0.04	<0.04	0.07	<0.04
K_2O	0.05	<0.04	<0.04	7.70	0.11 (25)	<0.04	<0.04	<0.04	<0.04
Total	98.99	98.65	99.20	97.19	98.47	98.86	98.83	98.68	97.93
					61141-56 (10–20 μm)				
SiO_2	44.4	0.07	37.8	74.2	44.5 (41)	53.6	52.6	51.0	44.9
TiO_2	0.05	52.9	0.10	0.17	0.88 (129)	0.72	0.80	1.15	0.84
Al_2O_3	34.6	<0.04	<0.04	11.7	23.9 (72)	1.05	1.05	1.39	0.97
Cr_2O_3	<0.04	0.44	0.06	<0.04	0.14 (12)	0.44	0.43	0.38	0.09
MgO	0.07	2.96	37.3	0.42	7.60 (448)	25.8	22.5	14.3	1.03
CaO	19.0	0.21	0.13	0.64	14.5 (33)	1.75	4.51	19.1	10.7
FeO	0.17	41.7	24.2	1.63	6.75 (445)	16.1	17.2	11.5	39.9
Na_2O	0.68	<0.04	<0.04	1.32	0.42 (38)	<0.04	<0.04	0.09	<0.04
K_2O	0.07	<0.04	<0.04	8.40	0.14 (26)	<0.04	<0.04	<0.04	<0.04
Total	99.04	98.28	99.59	98.48	98.75	99.46	99.09	98.91	98.43
					64801-82 (20–45 μm)				
SiO_2	44.1	0.06	37.7	73.5	45.5 (38)	53.3	51.4	50.8	48.6
TiO_2	<0.04	53.3	0.07	0.39	1.02 (143)	0.78	0.73	1.34	0.36
Al_2O_3	34.7	0.15	0.06	12.1	22.7 (78)	1.17	1.12	1.84	0.59
Cr_2O_3	<0.04	0.39	0.08	<0.04	0.13 (12)	0.41	0.36	0.56	0.24
MgO	<0.04	4.01	37.1	<0.04	6.97 (503)	26.1	19.6	15.3	5.40
CaO	19.3	0.22	0.15	0.93	13.9 (36)	1.84	4.75	18.5	19.3
FeO	0.07	40.4	24.1	1.64	7.02 (502)	15.5	20.6	10.4	23.9
Na_2O	0.47	<0.04	<0.04	0.93	0.42 (35)	<0.04	<0.04	0.09	0.08
K_2O	<0.04	0.04	<0.04	7.93	0.21 (58)	<0.04	<0.04	<0.04	<0.04
Total	98.64	98.57	99.26	97.42	97.97	99.10	98.56	98.83	98.47
					64801-82 (10–20 μm)				
SiO_2	43.9	0.04	37.7	70.8	44.8 (31)	53.5	52.4	50.6	48.4
TiO_2	<0.04	52.6	0.08	0.62	0.76 (98)	0.66	0.78	1.74	0.83
Al_2O_3	34.7	0.06	<0.04	12.7	23.8 (71)	1.18	1.15	2.14	1.20
Cr_2O_3	<0.04	0.56	0.08	<0.04	0.13 (13)	0.41	0.38	0.54	0.08
MgO	0.07	2.77	37.4	0.52	7.24 (460)	26.4	22.6	15.9	6.58
CaO	19.3	0.32	0.18	2.02	14.3 (34)	1.74	4.48	17.7	15.9
FeO	0.15	41.7	23.7	3.03	6.41 (446)	15.1	17.0	10.2	25.4
Na_2O	0.51	<0.04	<0.04	0.72	0.42 (47)	<0.04	<0.04	0.09	0.08
K_2O	<0.04	<0.04	<0.04	5.81	0.19 (46)	<0.04	<0.04	<0.04	<0.04
Total	98.63	98.05	99.14	96.22	98.09	98.99	98.79	98.91	98.47
					62231-91 (20–45 μm)				
SiO_2	43.7	0.07	37.7	71.6	44.5 (39)	53.1	52.1	50.8	47.8
TiO_2	<0.04	52.6	0.08	0.39	0.92 (111)	0.68	0.60	1.10	1.39
Al_2O_3	35.0	0.10	<0.04	13.7	23.0 (80)	0.89	0.98	1.39	1.69
Cr_2O_3	0.05	0.39	0.14	0.07	0.21 (19)	0.42	0.44	0.49	0.17
MgO	0.07	2.83	37.1	0.56	7.69 (546)	25.2	20.9	14.5	6.53
CaO	19.3	0.22	0.13	1.24	14.1 (36)	1.71	4.63	19.0	13.3
FeO	0.15	42.1	24.0	0.71	7.26 (490)	16.8	19.1	11.2	27.9
Na_2O	0.50	<0.04	<0.04	1.19	0.41 (31)	<0.04	<0.04	0.07	0.05
K_2O	0.04	0.04	<0.04	7.51	0.15 (22)	<0.04	<0.04	<0.04	<0.04
Total	98.81	98.31	99.15	96.97	98.20	98.80	98.75	98.55	98.83
					62231-91 (10–20 μm)				
SiO_2	44.2	0.08	37.4	68.2	44.4 (37)	53.3	52.6	51.3	47.6
TiO_2	<0.04	52.7	0.09	0.20	0.91 (132)	0.59	0.74	1.17	1.36
Al_2O_3	34.8	0.06	<0.04	15.4	23.0 (76)	0.98	1.09	1.55	1.58
Cr_2O_3	<0.04	0.51	0.08	<0.04	0.18 (14)	0.39	0.41	0.46	0.13
MgO	0.06	3.24	35.2	0.16	7.66 (464)	24.2	21.9	14.8	6.09
CaO	19.2	0.33	0.17	1.52	14.2 (35)	1.69	4.43	18.2	13.8
FeO	0.11	41.2	26.5	1.37	7.34 (527)	18.0	18.1	11.6	28.0
Na_2O	0.53	<0.04	<0.04	1.11	0.45 (53)	<0.04	<0.04	0.08	0.04
K_2O	0.05	<0.04	<0.04	9.40	0.14 (29)	<0.04	<0.04	<0.04	<0.04
Total	98.95	98.12	99.44	97.36	98.29	99.15	99.27	99.16	98.60

[a]Maturity as I_s/FeO of the <250 μm fraction [*Morris*, 1978] is given directly after the soil number, a value commonly used as the reference maturity for an entire soil. Values in brackets are the 2 sigma error.

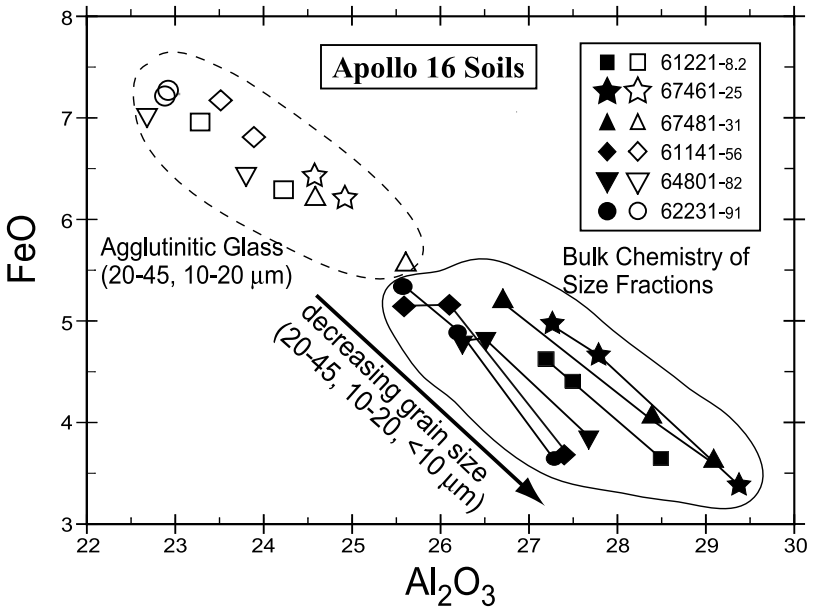

Figure 3. Comparison of chemistry of the agglutinitic glass with the bulk chemistry of the three soil size fractions for Apollo 16 highland soils. Modified from LPSC abstract [*Taylor et al.*, 2003].

significantly. This is indicated by the large increase in I_S/FeO values with decreasing grain size (Figure 2), not proportionate to the much smaller increases in the abundances of agglutinitic glass, similar to in the mare soils [*Taylor et al.*, 2001b].

5. Mineral and Glass Chemistry

[20] As part of our extensive characterization of the fine grain sizes of highland soils, we have determined the average compositions of each of the several phases in the three size fractions. In Table 5, we have presented these compositions for the 20–45 and 10–20 μm fractions of the soils. The precisions associated with these averages are quite large, and we have included the 2σ precisions for the agglutinitic glasses, which are by far the largest of all. This illustrates the general findings of several studies of agglutinitic glass in that the compositions actually range between pure plagioclase and that of the mafic minerals, olivine and pyroxene [e.g., *Hu and Taylor*, 1977]. As shown in Figure 3, comparison of the average composition of the agglutinitic glass in the different size fractions of a given soil are approximately constant, particularly when the precisions are taken into consideration.

[21] With the mare soils [*Taylor et al.*, 2001b], the compositions of the 20–45, 10–20, and <10 μm fractions became progressively similar to the agglutinitic glass, with the glass being higher in plagioclase components (i.e., CaO, Al_2O_3). However, the agglutinitic glass for the highland soils does not demonstrate such a well-defined trend. In fact, the progression from coarse to fine fractions has the composition of the size fractions becoming more plagioclase rich, but the agglutinitic glass becomes enriched slightly but distinctly in the mafic components (e.g., FeO, MgO), as illustrated in Figure 3. Although the standard deviation of the average agglutinitic glass compositions is large, the data for highland soils are systematic. These unexpected results, in contrast to those for the mare soils, would appear to indicate that either the F^3 model does not adequately explain the formation of the highland soils or some other process, such as an addition of a mare component, has been operative.

[22] A perplexing aspect of the chemical data for the highland soils is present when comparing TiO_2 contents of the size separates compared to that of the agglutinitic glass, similar to that for Ti-rich soils [*Taylor et al.*, 2001a, 2001b]. Although ilmenite is present in the finest fractions of mare soils in proportions correlated to the type of basalt, the agglutinitic glass was observed to be depleted in TiO_2 by more than a factor of two; strongly suggesting ilmenite did not enter the glass in proportion to its abundance in basaltic soils [*Pieters et al.*, 2002].

[23] However, the opposite occurs with highland soils. As shown dramatically in Figure 4, the TiO_2 contents of the Apollo 16 agglutinates are distinctly enriched compared to the chemistry of the size fractions of the soils. In fact, it is not only the TiO_2 contents. The chemistry of the highland agglutinates in Figure 4, as taken from Table 5, shows that for the Apollo 16 soils, the agglutinitic glass has a distinct enrichment in TiO_2, Cr_2O_3, MgO, FeO, and K_2O, compared to the bulk chemistry of each size fraction. This strongly supports the paradigm that there has been large-scale mixing between mare and highlands [*Pieters and Taylor*, 2003a]. But, it was the glass component of the maria that appears to have been selectively added to the Apollo 16 site. This may well have masked the possible fusion of the finest fraction effects.

6. Visible to Near-Infrared Spectroscopy of Highland Soils

[24] Bidirectional reflectance spectra for the bulk soil and size separates are shown for all Apollo 14 and 16 soils in

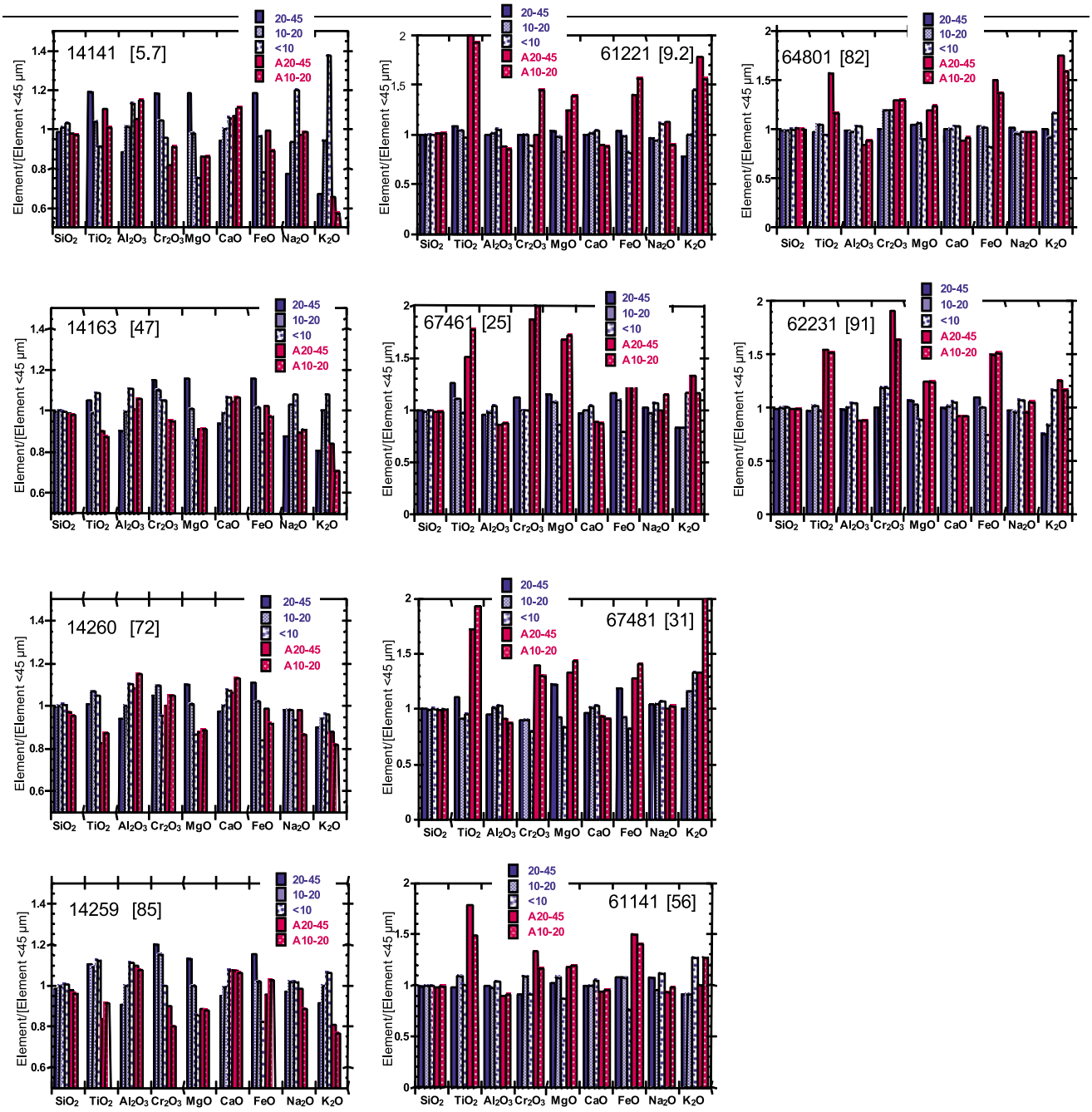

Figure 4. Chemistry of soil components relative to the chemistry of the bulk soil (<45 μm) for representative highland soils. The first three bars (blue shades) are the composition of three soil size separates (see legend). These are followed by the average composition of agglutinitic glass (red shades) present in the indicated size separate. The number in brackets is the I_s/FeO value for the bulk soil from *Morris* [1978]. Some of these data have been reported by *Pieters and Taylor* [2003a].

Figure 5. The presence of np-Fe^0 both in the agglutinitic glass and on the surfaces of grains greatly affects the optical properties of materials exposed to the space environment [e.g., *Hapke*, 2001; *Noble et al.*, 2001, 2007]. The least weathered soils (14141 and 61221) exhibit the most prominent absorption bands diagnostic of the mafic minerals present, largely low-calcium pyroxene. The finest fraction not only contains the lowest abundance of mafic minerals (Table 2), but it also contains the highest proportion of np-Fe^0 (Figure 2). Diagnostic absorptions are weak or nonexistent in the finest fraction. Similarly, coarse-grained separates contain fewer agglutinates, proportionately greater mafic minerals, and have smaller surface to volume ratios than the finer grained separates. Coarse-grained separates thus always exhibit more prominent absorption bands than fine-grained separates from the same soil sample.

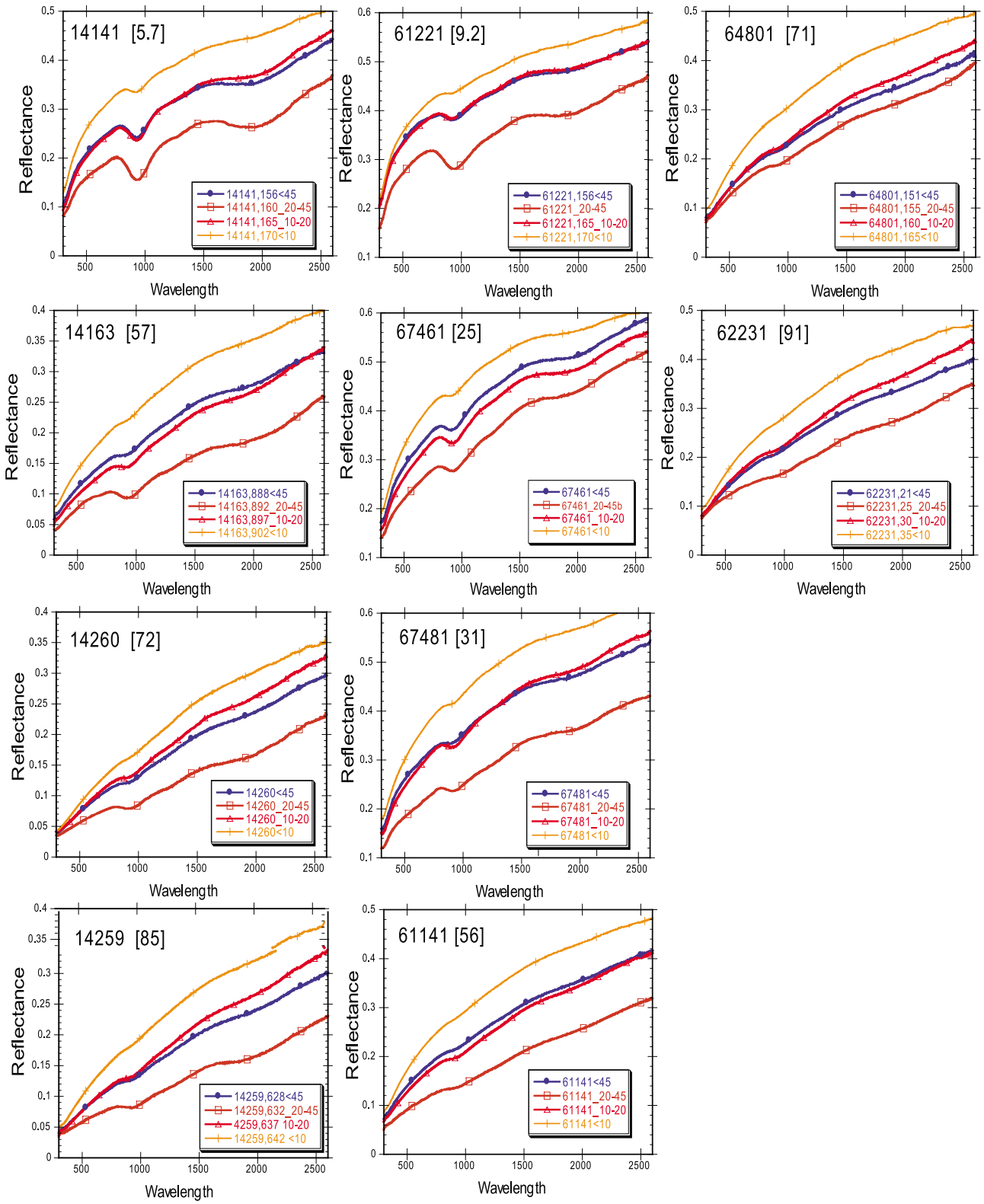

Figure 5. Bidirectional reflectance spectra of LSCC highland soils. Data for 64801 are from *Pieters and Taylor* [2003a].

[25] There is considerable variation of the composition of different size fractions for the same soil (e.g., Figure 2), and it is difficult to reliably quantify the bulk mineralogy for a given soil. Most abundance analyses are performed on limited amounts of size fraction, and these data must be used with caution as representations of a soil as a whole. Nevertheless, based on the close similarity of spectra for the 10–20 μm size fraction with the bulk soil seen across

Figure 5, this size fraction appears to capture a good balance of diverse competing soil processes. We thus recommend the 10–20 μm size fraction be used as a proxy for the bulk when measurements are impractical or impossible for the bulk soil.

7. Discussion

[26] The chemistries of the bulk soil size fractions of the highland soils have similar trends as compared to those of the mare soils. With decreasing grain size, the soil compositions become enriched in plagioclase (CaO, Al_2O_3) and depleted in mafic components (FeO, MgO). The same general trends also exist for both the mare and highland soils with respect to the modal mineral and glass abundances. As with the mare soils, the large increases in the I_S/FeO values, with decrease in grain size, are not proportional to the more minor increases in abundances of the agglutinitic glasses. This large increase in I_S/FeO is attributed to np-Fe^0 that accumulates on the surfaces of the soil particles, as discussed for mare soils [*Hapke*, 2001; *Noble et al.*, 2001; *Pieters et al.*, 2000, 2001; *Taylor et al.*, 2001a, 2001b; *Keller and McKay*, 1997; *Keller et al.*, 2000; *Wentworth et al.*, 1999].

[27] In addition, the unexpected enrichment of the highland agglutinitic glass in mafic components, compared to the compositions of the bulk soil fractions for Apollo 16 highland soils, has necessitated reconsideration of operative processes for the evolution of lunar soils, previously addressed by *Pieters and Taylor* [2003a]. In particular, the role of selective comminution, lateral mixing, and preferential melting of local components are all clearly important. The suspected large-scale mixing between mare and highlands may be real; however, it is the glass chemistry of the mare that is preferentially added to the highlands (i.e., TiO_2, Cr_2O_3, MgO, FeO, and K_2O). The regolith differential melting sequence, for both highland and mare soils, would appear to be: glass > plagioclase > pyroxene $\gg$ ilmenite. Furthermore, it would seem that lunar mafic-rich glass is more likely to melt than Al-rich glass, since mare soils tend to accumulate a higher overall abundance of agglutinitic glass than highland soils [*Taylor et al.*, 2001a, 2001b, 2003]. Couple this with the fact that the finer portions of the soil, the ones with dominant agglutinitic glass, are ballistically transported greater distances by impact processes, perhaps enhanced by electrostatic levitation [*Farrell et al.*, 2008]. With these considerations in mind, one can readily explain the mare additive to form the FeO-MgO enriched agglutinitic glass of the Apollo 16 highlands.

[28] Although we suggest that the source of the mafic glass component in highland soils is the maria in origin, an alternate source for the Apollo 16 soils might be the abundant ''mafic impact melt breccias'' thought to be derived from Imbrium [*Korotev*, 1997]. But, here we find it difficult to address the scenario that these melt breccias were selectively and preferentially incorporated into the Apollo 16 agglutinitic glass. Indeed, the Apollo 14 soil chemistry appears to reflect this possible Imbrium component, as seen from their higher K phase (Figure 1). However, the model we prefer is necessarily dependent on the small number of sites for which samples are available. It is obvious that we need samples from a highland site far removed from any maria.

8. Summary

[29] The reflectance spectroscopy of the surface of any airless body only sees the properties of the fine-grained regolith, the dust. The <45 μm portions of carefully selected Apollo highland soils of the Moon have been characterized both mineralogically and chemically as ''ground truth'' for this airless body (mare soils have been previously reported by *Taylor et al.* [2001b]). There is a general increase in agglutinitic glass content and I_S/FeO values with decreasing grain size for the highland soils, exactly the same as with the mare soils. However, the increase in I_S/FeO with decreasing grain size is far greater than the increase in abundance of agglutinitic glass; this is evidence of an additional source of np-Fe^0 as vapor-deposited rims on particle surfaces [e.g., *Hapke et al.*, 1975].

[30] The increase in plagioclase chemical components with decreasing grain size of the agglutinitic glass chemistry, very typical for mare soils, is not obvious for these Apollo 16 highland soils. Instead, Apollo 16 agglutinitic glass chemistry contains more mafic ''mare soil components'' than the bulk soil chemistry. It is reasoned that the Apollo 16 soils have experienced additions of impact-transported soil components from nearby surrounding mare terrains. Therefore, the adulterated nature of the highland soils near mare terrains may differ slightly from those highland soils more remotely located, e.g., northern farside.

[31] **Acknowledgments.** We would like to thank CAPTEM for the allocation of the pristine suite of highland soils. The Curatorial Staff at Johnson Space Center are also thanked for their efficient handling of the distribution of the numerous size fractions of the lunar soils, including the production of the polished grain mounts. We have benefited from fruitful discussions over the years with Paul Lucey, A. Basu, Sarah Noble, Jim Papike, Amy Riches, and Yang Liu. In addition, it has been the thorough reviews by A. Basu and Sarah Noble that have been extremely helpful in substantially improving this paper. RELAB at Brown University is a multiuser facility supported under NAG 5-3871. The research presented in this paper was supported by NASA grants from the Cosmochemistry Program to each of the members of the Lunar Soil Characterization Consortium (LSCC), for which we are collectively appreciative.

References

Basu, A., and E. Molinaroli (1999), Sediments of the Moon and Earth as end-members for comparative planetology, *Earth Moon Planets*, *85–86*, 25–43, doi:10.1023/A:1017018621548.

Basu, A., D. S. McKay, R. V. Morris, and S. J. Wentworth (1996), Anatomy of individual agglutinates from a lunar highland soil, *Meteorit. Planet. Sci.*, *31*, 777–782.

Farrell, W. M., T. J. Stubbs, G. T. Delory, R. R. Vondrak, M. R. Collier, J. S. Halekas, and R. P. Lin (2008), Concerning the dissipation of electrically charged objects in the shadowed lunar polar regions, *Geophys. Res. Lett.*, *35*, L19104, doi:10.1029/2008GL034785.

Hapke, B. (2001), Space weathering from Mercury to the asteroid belt, *J. Geophys. Res.*, *106*, 10,039–10,073, doi:10.1029/2000JE001338.

Hapke, B., W. A. Cassidy, and E. N. Wells (1975), Effects of vapor-phase deposition processes on the optical, chemical, and magnetic properties of the lunar regolith, *Earth Moon Planets*, *13*, 339–353, doi:10.1007/BF00567525.

Hu, H. N., and L. A. Taylor (1977), Lack of chemical fractionation in major and minor elements during agglutinate formation, *Proc. Lunar Planet. Sci. Conf., 8th*, 3645–3656.

Keller, L. P., and D. S. McKay (1997), The nature and origin of rims on lunar soil grains, *Geochim. Cosmochim. Acta*, *61*, 2331–2340, doi:10.1016/S0016-7037(97)00085-9.

Keller, L. P., S. J. Wentworth, D. S. McKay, L. A. Taylor, C. M. Pieters, and R. V. Morris (2000), Space weathering in the fine size fraction of lunar soils: Mare/highland differences, *Lunar Planet. Sci.* [CD-Rom], *XXXI*, Abstract 1655.

Korotev, R. L. (1997), Some things we can infer about the Moon from the composition of the Apollo 16 regolith, *Meteorit. Planet. Sci.*, *32*, 447–478.

McGee, J. J. (1993), Lunar ferroan anorthosites' mineralogy, compositional variations, and petrogenesis, *J. Geophys. Res.*, *98*, 9089–9105, doi:10.1029/93JE00400.

Morris, R. V. (1976), Surface exposure indices of lunar soils: A comparative FMR study, *Proc. Lunar Planet Sci. Conf., 7th*, 315–335.

Morris, R. V. (1978), The surface exposure (mature) of lunar soils: Some concepts and Is/FeO compilation, *Proc. Lunar Planet. Sci. Conf., 9th*, 2287–2297.

Noble, S. K., C. M. Pieters, L. A. Taylor, R. V. Morris, C. C. Allen, D. S. McKay, and L. P. Keller (2001), The optical properties of the finest fraction of lunar soil: Implications for space weathering, *Meteorit. Planet. Sci.*, *36*, 31–42.

Noble, S. K., C. M. Pieters, and L. P. Keller (2007), An experimental approach to understanding the optical effects of space weathering, *Icarus*, *192*, 629–642, doi:10.1016/j.icarus.2007.07.021.

Papike, J. J., S. B. Simon, C. White, and J. C. Laul (1982), The relationship of the lunar regolith <10 μm fraction and agglutinates, part I: A model for agglutinate formation and some indirect supportive evidence, *Proc. Lunar Planet. Sci. Conf., 12th*, 409–420.

Pieters, C. M. (1983), Strength of mineral absorption features in the transmitted component of near-infrared reflected light: First results from RELAB, *J. Geophys. Res.*, *88*, 9534–9544, doi:10.1029/JB088iB11p09534.

Pieters, C. M. (1993), Compositional diversity and stratigraphy of the lunar crust derived from reflectance spectroscopy, in *Remote Geochemical Analysis: Elemental and Mineralogical Composition*, edited by C. M. Pieters and P. A. J. Englert, pp. 309–339, Cambridge Univ. Press, New York.

Pieters, C. M., and L. A. Taylor (2002), The perplexing role of TiO2 in the evolution of lunar soil, *Lunar Planet. Sci.* [CD-ROM], *XXXIII*, Abstract 1886.

Pieters, C. M., and L. A. Taylor (2003a), Systematic global mixing and melting in lunar soil evolution, *Geophys. Res. Lett.*, *30*(20), 2048, doi:10.1029/2003GL018212.

Pieters, C. M., and L. A. Taylor (2003b), The role of agglutinates in lunar highland soil formation, *Lunar Planet. Sci.* [CD-ROM], *XXXIV*, Abstract 1223.

Pieters, C. M., E. M. Fischer, O. Rode, and A. Basu (1993), Optical effects of space weathering: The role of the finest fraction, *J. Geophys. Res.*, *98*, 20,817–20,824, doi:10.1029/93JE02467.

Pieters, C. M., L. A. Taylor, S. K. Noble, L. P. Keller, B. Hapke, R. V. Morris, C. C. Allen, and S. Wentworth (2000), Space weathering on airless bodies: Resolving a mystery with lunar samples, *Meteorit. Planet. Sci.*, *35*, 1101–1107.

Pieters, C. M., D. G. Stankevich, Y. G. Shkuratov, and L. A. Taylor (2001), Statistical analysis of lunar mare soil mineralogy, chemistry, and reflectance spectra, *Lunar Planet. Sci.* [CD-Rom], *XXXII*, Abstract 1783.

Pieters, C. M., D. G. Stankevich, Y. G. Shkuratov, and L. A. Taylor (2002), Statistical analysis of the links among lunar mare soil mineralogy, chemistry, and reflectance spectra, *Icarus*, *155*, 285–298, doi:10.1006/icar.2001.6749.

Taylor, L. A., and D. S. McKay (1992), Beneficiation of lunar rocks and regolith: Concepts and difficulties, in *Engineering, Construction, Operations in Space III*, vol. 1, edited by W. Sadeh et al., pp. 1058–1069, Am. Soc. of Civ. Eng., New York.

Taylor, L. A., A. Patchen, D.-H. Taylor, J. G. Chambers, and D. S. McKay (1996), X-ray digital imaging and petrography of lunar mare soils: Data input for remote sensing calibrations, *Icarus*, *124*, 500–512, doi:10.1006/icar.1996.0226.

Taylor, L. A., C. M. Pieters, R. V. Morris, L. P. Keller, D. S. McKay, A. Patchen, and S. J. Wentworth (1999), Integration of the chemical and mineralogical characteristics of lunar soils with reflectance spectroscopy, *Lunar Planet. Sci.* [CD-Rom], *XXX*, Abstract 1859.

Taylor, L. A., C. M. Pieters, L. P. Keller, R. V. Morris, D. S. McKay, A. Patchen, and S. J. Wentworth (2001a), The effects of space weathering on Apollo 17 mare soils: Petrographic and chemical characterization, *Meteorit. Planet. Sci.*, *36*, 288–299.

Taylor, L. A., C. M. Pieters, L. P. Keller, R. V. Morris, and D. S. McKay (2001b), Lunar mare soils: Space weathering and the major effects of surface-correlated nanophase Fe, *Geophys. Res. Lett.*, *106*, 27,985–27,999.

Taylor, L. A., J. T. Cahill, A. Patchen, C. Pieters, R. V. Morris, L. P. Keller, and D. S. McKay (2001c), Mineralogical and chemical characterization of lunar highland regolith: Lessons learned from mare soils, *Lunar Planet. Sci.* [CD-ROM], *XXXII*, Abstract 2196.

Taylor, L. A., A. Patchen, J. Cahill, C. M. Pieters, R. V. Morris, L. P. Keller, and D. S. Mckay (2002), Mineral and glass characterization of Apollo 14 soils, *Lunar Planet. Sci.* [CD-ROM], *XXXIII*, Abstract 1302.

Taylor, L. A., C. M. Pieters, A. Patchen, D.-H. Taylor, R. V. Morris, L. P. Keller, and D. S. McKay (2003), Mineralogical characterization of lunar highland soils, *Lunar Planet. Sci.* [CD-ROM], *XXXIV*, Abstract 1774.

Wentworth, S. J., L. P. Keller, D. S. McKay, and R. V. Morris (1999), Space weathering on the Moon: Patina on Apollo 17 samples 75075 and 76015, *Meteorit. Planet. Sci.*, *34*, 593–603.

L. P. Keller, D. S. McKay, and R. V. Morris, NASA Johnson Space Center, Code KR, Houston, TX 77058, USA.

A. Patchen, D.-H. S. Taylor, and L. A. Taylor, Planetary Geosciences Institute, Department of Earth and Planetary Sciences, University of Tennessee, Knoxville, TN 37996, USA. (lataylor@utk.edu)

C. Pieters, Department of Geological Sciences, Brown University, Providence, RI 02912, USA.